Journal of Medicinal Chemistry

Article

pubs.acs.org/jmc

Structure−Activity Relationship of Nonacidic Quinazolinone Inhibitors of Human Microsomal Prostaglandin Synthase 1 (mPGES 1)

Florian Rörsch,*[,†] Estel.la Buscató,[‡] Klaus Deckmann,[†] Gisbert Schneider,[§] Manfred Schubert-Zsilavecz,[‡] Gerd Geisslinger,[†] Ewgenij Proschak,[‡] and Sabine Grösch[†]

[†]Johann Wolfgang Goethe-University, Institute of Clinical Pharmacology, *pharmazentrum frankfurt*, LiFF/ZAFES, Theodor-Stern-Kai 7, D-60590 Frankfurt/Main, Germany

[‡]Johann Wolfgang Goethe-University, Institute of Pharmaceutical Chemistry, LiFF/ZAFES, Max-von-Laue-Strasse 9, D-60438 Frankfurt/Main, Germany

[§]ETH Zürich, Department of Chemistry and Applied Biosciences, Wolfgang-Pauli-Strasse 10, CH-8093 Zürich, Switzerland

Supporting Information

ABSTRACT: Microsomal prostaglandin E synthase 1 (mPGES-1) is a key enzyme of the arachidonic acid cascade. Its product PGE_2 plays an important role in various inflammatory processes, pain, fever, and cancer. Selective inhibition of mPGES-1 might be a promising step to avoid cyclooxygenase-related effects of NSAIDs. We studied a class of quinazolinone derivatives of the lead structure FR20 for their effects on the isolated human and murine enzymes, human HeLa cells, and in various settings of the whole blood assay. Novel compounds with direct enzyme inhibiting activity in the submicromolar range (IC_{50}: 0.13−0.37 μM) were designed using a bioisosteric replacement strategy and proved to be effective in both cells and human whole blood. Furthermore, pharmacological profiling of toxicity and eicosanoid screening with LC/MS-MS was applied to characterize this new class of mPGES-1 inhibitors.

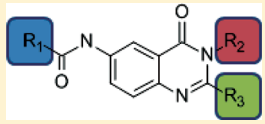

INTRODUCTION

The microsomal prostaglandin E_2-synthase 1 (mPGES-1) is an inducible enzyme of the arachidonic acid cascade and mainly coupled to the expression of cyclooxygenase-2 (COX-2).[1] Proinflammatory stimuli such as lipopolysaccharide (LPS) up-regulate the protein level of both enzymes. The major product, prostaglandin E_2 (PGE_2), plays an important role in the mediation of pain,[2,3] fever,[4] the development of various cancer types,[5] and several inflammatory diseases like rheumatoid arthritis.[6] Besides clinically relevant diseases, PGE_2 is involved in gastrointestinal protection[7,8] and the onset of wakefulness and maintenance of the circadian rhythm.[9] PGE_2 production is inhibited by nonsteroidal anti-inflammatory drugs (NSAIDs), specifically selective and nonselective COX-inhibitors. Inhibition of mPGES-1 might improve the pharmacological profile of current analgesic, anti-inflammatory, and antipyretic medication due to a reduction of side effects as compared to known NSAIDs.[10,11] Especially patients under continuous long-term treatment with NSAIDs may suffer from gastrointestinal ulcers and cardiovascular complications.[12,13] Permanent treatment, however, is indicated for treatment of chronic inflammatory diseases like rheumatoid arthritis (RA) or arteriosclerosis. Several mPGES-1 inhibitors have been tested in vitro and in vivo in different disease models (Chart 1).[14]

For mPGES-1 inhibition, two main approaches have been pursued. On the one hand, mPGES-1 can be inhibited via down-regulation of mPGES-1 expression. Benzothiophene γ-hydroxybutenolide (BTH) **1** significantly reduced PGE_2 levels in the mouse air pouch and collagen-induced arthritis (CIA) models.[15] On the other hand, mPGES-1 activity is directly affected by small-molecule inhibitors. AF3442 **2** inhibited mPGES-1 activity in LPS-stimulated human monocytes and human whole blood.[16] PF-9184 **3** exhibits high potency on recombinant human mPGES-1 with an IC_{50} of 16.5 nM but loses its potency on the rat mPGES-1 in vitro (IC_{50} of 1080 nM on recombinant rat mPGES-1) and in vivo (no effect in rat air pouch model).[17] A series of phenanthrene imidazole inhibitors around the lead compound MF63 **4** also showed high potency on the human and guinea pig enzyme and in the human whole blood assay with selectivity over several other related enzymes but lacks the ability to inhibit mouse or rat mPGES-1.[18]

These data illustrate one main problem occurring during the development of selective human mPGES-1 inhibitors, as they are inactive regarding the inhibition of the mouse or rat mPGES-1, thus rendering the application of preclinical animal models impossible. This species difference is due to several amino acid exchanges between the human and murine enzyme, leading to variations in the active site of mPGES-1. Several dual 5-lipoxygenase (5-LO)/mPGES-1 inhibitors extend the pharmacological profile of anti-inflammatory agents and exhibit activity in animal models of carrageenan-induced rat pleurisy and aortic aneurysm.[19−22] In addition, natural compounds like arzanol **5** from *Helichrysum italicum* have been reported to affect inflammation and PGE_2 levels in carrageenan-induced pleurisy in rats.[23] We recently reported a series of novel

Received: December 14, 2011
Published: March 26, 2012

Chart 1. Several Published mPGES-1 Inhibitors

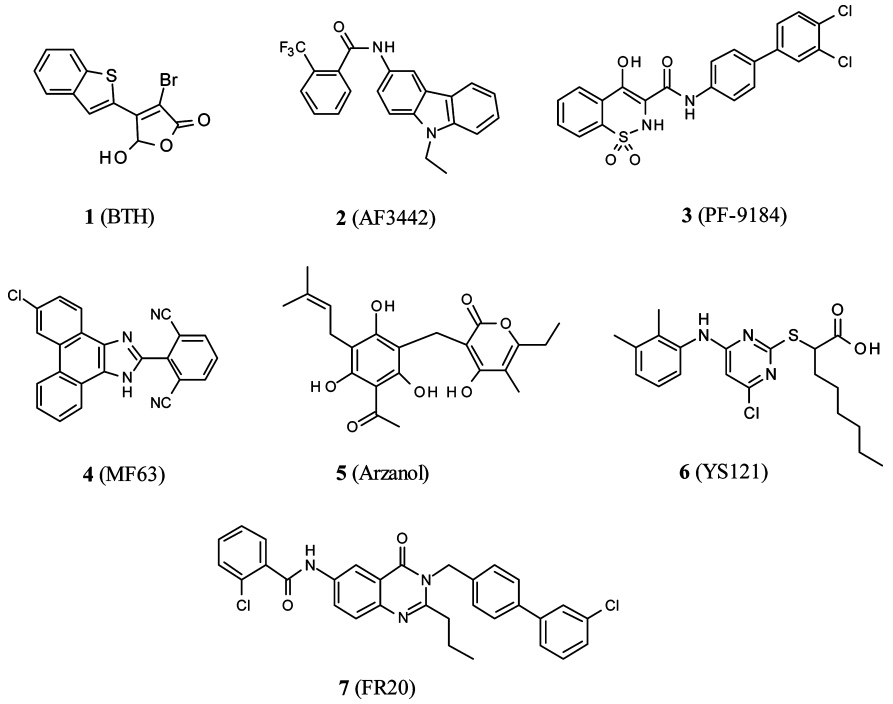

Scheme 1. Schematic Synthesis Route for Compounds Based on a Quinazolinone Scaffold[a]

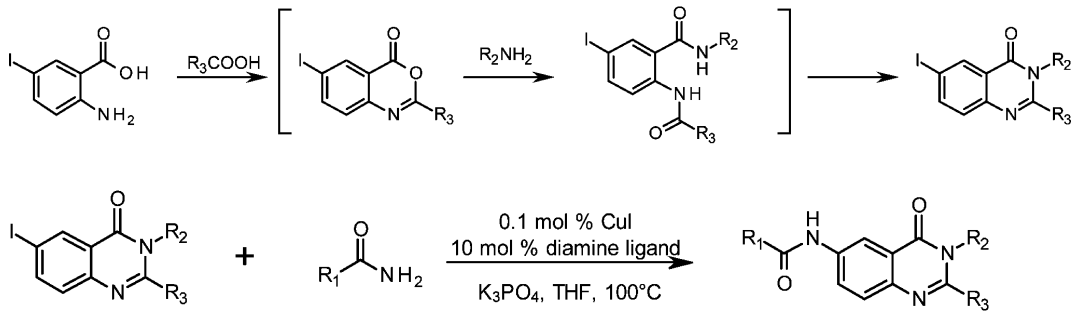

[a]Formation of 2,3-disubstituted 3*H*-quinazolin-4-one is followed by the formation of the final product by a related Goldberg reaction.

nonacidic mPGES-1 inhibitors that were found by a multistep virtual screening protocol.[24] Quinazolinone **7** (FR20) provided the starting point for an extensive structure–activity relationship study (SAR). Here we present a structure optimization approach including chemical synthesis of quinazolinone derivatives, detailed information about activity on human and murine isolated mPGES-1 enzyme, in vitro nonspecific cellular toxicity, and impact on different eicosanoids in human whole blood. As a major outcome of this study, we present a class of direct human mPGES-1 inhibitors with low nonspecific cellular toxicity and a broad whole blood eicosanoid profile.

RESULTS

Assembly of the Quinazolinone Compound Library and Development of a Synthesis Route. On the basis of the reference structure **7**, several derivatives (**7a**–**7n**, **7r**–**7x**) were purchased from Asinex (www.asinex.com, Moscow, Russia). Three novel derivatives (**7o**, **7p**, **7q**) were synthesized (Scheme 1) to extend the chemical diversity and provide a synthesis route for this scaffold class. All compounds are listed in Chart 2.

Human mPGES-1 Activity Screening. To investigate the inhibitory potency of these substances on the human mPGES-1, we compared the inhibition rate of each derivative at 1 μM on isolated protein in the mPGES-1 activity assay with the reference structure **7** (Table 1). Derivatives **7f**, **7i**, **7k**, **7l**, **7n**, **7o**, **7q**, and **7r** equipotently reduced the PGE_2-level ±5% or higher as compared to **7**. For those substances, dose–response curves (exemplary curve in Supporting Information Figure S1) and IC_{50} values with 95% confidence intervals were calculated. IC_{50} values were between 0.13 μM (**7**) and 0.37 μM (Table 1). IC_{50} values of these derivatives reveal comparable potencies.

Murine mPGES-1 Activity Screening. Because the human and murine mPGES-1 differ in their amino acid sequences, we further investigated the influence of **7** and equipotent derivatives **7f**, **7i**, **7k**, **7l**, **7n**, **7o**, **7q**, and **7r** on murine mPGES-1 in vitro. The compounds were tested on the murine mPGES-1 enzyme in the microsomal fraction of two different cell types. Mouse macrophage cells (RAW) and mouse fibroblast cells (NIH-3T3) were stimulated with either LPS or IL-1β/TNFα to upregulate mPGES-1 protein levels. Protein extracts were incubated with different concentrations of quinazolinone series compounds or the mouse mPGES-1

dx.doi.org/10.1021/jm201687d | *J. Med. Chem.* 2012, 55, 3792–3803

Chart 2. Twenty-Four Derivatives around the Lead Structure 7 Were Used for Structure–Activity Relationship Studies and Pharmacological Profiling[a]

Identifier	Structure
	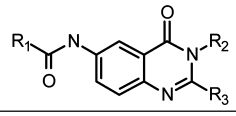
7	R_1 = 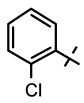 R_2 = 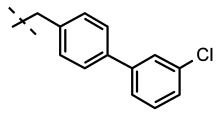 R_3= Propyl
7a	R_1 = 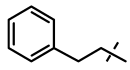 R_2 = 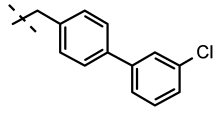 R_3= Propyl
7b	R_1 =  R_2 = 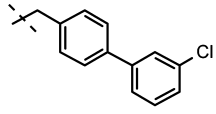 R_3= Propyl
7c	R_1 = 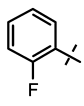 R_2 = 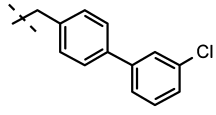 R_3= Propyl
7d	R_1 = CH_3 R_2 = 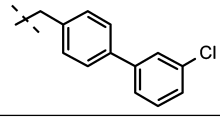 R_3= Propyl
7e	R_1 = *tert*-Butyl R_2 = 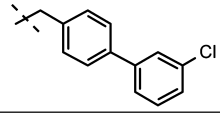 R_3= Propyl
7f	R_1 = 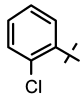 R_2 = 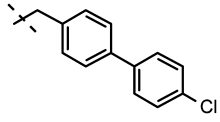 R_3= Propyl
7g	R_1 =  R_2 = 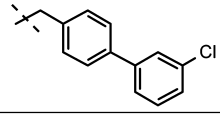 R_3= Propyl
7h	R_1 = 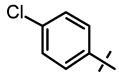 R_2 = 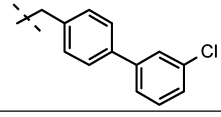 R_3= Propyl
7i	R_1 = 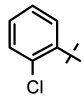 R_2 = 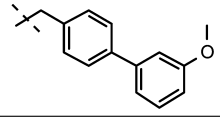 R_3= Propyl
7j	R_1 = 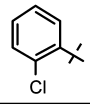 R_2 = 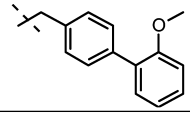 R_3= Propyl
7k	R_1 = 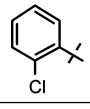 R_2 = 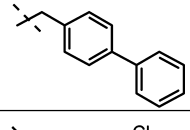 R_3= Propyl
7l	R_1 = 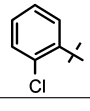 R_2 = 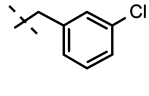 R_3= Propyl

dx.doi.org/10.1021/jm201687d | J. Med. Chem. 2012, 55, 3792–3803

Chart 2. continued

Identifier	Structure
	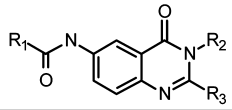
7**m**	R_1 = 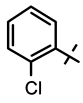 R_2 = 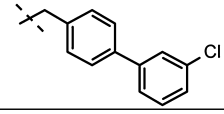 R_3= CH_3
7**n**	R_1 = 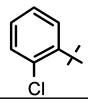 R_2 = 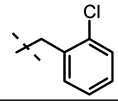 R_3= Propyl
7**o**	R_1 = 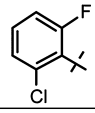 R_2 = 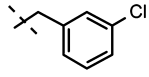 R_3= Propyl
7**p**	R_1 = 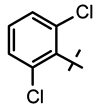 R_2 = 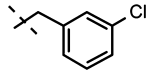 R_3= Propyl
7**q**	R_1 =  R_2 = 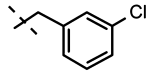 R_3= Propyl
7**r**	R_1 = 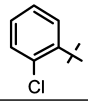 R_2 = 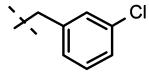 R_3= 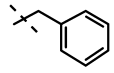
7**s**	R_1 =  R_2 = 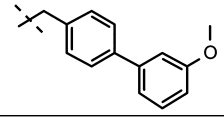 R_3= Propyl
7**t**	R_1 =  R_2 = 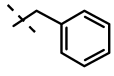 R_3= 
7**u**	R_1 = 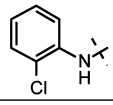 R_2 = 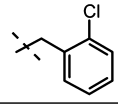 R_3= Propyl
7**v**	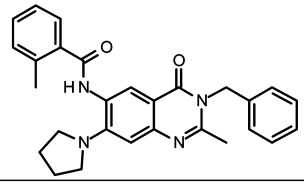
7**w**	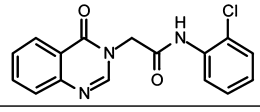
7**x**	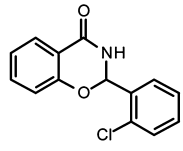

[a]Three additional compounds (**7v–x**) with slight variations were added.

inhibitor control substance **6** (YS121).[21] Neither RAW- nor NIH-derived mPGES-1 activity was impaired by quinazolinone compounds by more than 20% (Table 1), while **6** reduced the activity by more than 62%.

dx.doi.org/10.1021/jm201687d | *J. Med. Chem.* 2012, 55, 3792–3803

Table 1. Measured Activity of the Quinazolinone Series on Isolated Human and Murine (from RAW and NIH Cells) Enzyme at 1 μM Final Concentration with Standard Error of the Mean (SEM)[a]

	human				murine					
identifier unit	mPGES-1 inhibition @ 1 μM [%]	SEM [%]	IC_{50} [μM]	95% confidence interval [μM]	RAW mPGES-1 inhibition @ 1 μM [%]	SEM [%]	NIH mPGES-1 inhibition @ 1 μM [%]	SEM [%]	COX-1 inhibition @ 1 μM [%]	COX-2 inhibition @ 1 μM [%]
7	66.7	4.8	0.13	0.08−0.18	8.4	3.6	10.7	7.2	≤0	6.7
7a	32.7	6.6								
7b	15.3	6.0								
7c	30.0	4.6								
7d	14.8	5.8								
7e	18.8	10.1								
7f	**68.8**	3.1	**0.18**	0.10−0.32	12.4	3.4	17.1	2.2	2.6	≤0
7g	15.6	10.7								
7h	14.7	2.6								
7i	**71.5**	3.6	**0.21**	0.13−0.33	15.3	4.2	4.6	4.6	20.1	2.5
7j	61.3	8.4								
7k	**74.2**	0.9	**0.22**	0.13−0.38	11.8	3.5	20.3	1.9	8.4	5.8
7l	**86.3**	1.7	**0.36**	0.17−0.77	9.5	3.5	−0.8	4.5	≤0	≤0
7m	41.9	0.8								
7n	**83.6**	0.8	**0.18**	0.11−0.29	15.2	7.5	6.6	6.0	16.1	≤0
7o	**75.6**	1.3	**0.37**	0.26−0.53	−8.7	1.3	10.0	5.0	≤0	≤0
7p	61.3	2.3								
7q	63.1	3.9	**0.26**	0.16−0.42	6.0	2.3	0.9	1.5	≤0	≤0
7r	**67.2**	5.2	nd[b]		3.8	5.1	17.8	2.8	≤0	≤0
7s	15.9	7.2								
7t	≤0	16.1								
7u	14.1	13.2								
7v	37.1	10.7								
7w	≤0	22.8								
7x	≤0	7.0								
YS121					66.2 (@ 5 μM)	2.8	62.9 (@ 5 μM)	2.2		

[a]The 50% inhibitory concentration (IC_{50}) on human enzyme was calculated for each derivative showing larger inhibitory potency at 1 μM than the lead structure **7**. With 95% percent probability the IC_{50} is in the given range of the confidence interval. Cross-reactivity against COX-1/COX-2 enzymes with 1 μM inhibitor concentration was measured in vitro. Data are the mean of $n \geq 3$. [b]nd = not determined.

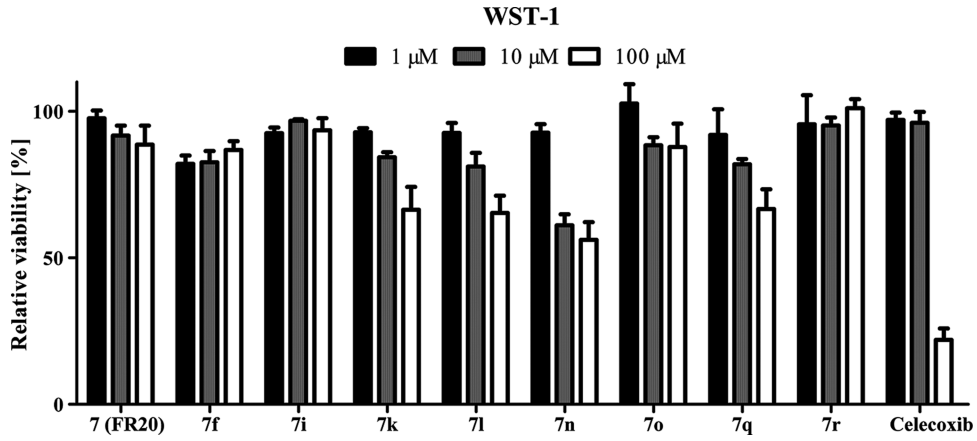

Figure 1. Cell viability assay with FR20 series compounds on stimulated human HeLa cells. Cell viability is given as percent of DMSO control with SEM after 24 h of incubation ($n \geq 3$).

COX-1 and COX-2 Cross-Reactivity. Cross-reactivity of these compounds against both COX-isoforms was tested in vitro. Neither COX-1 nor COX-2 was inhibited by any compound by more than 20% at 1 μM inhibitor concentration (Table 1).

Toxicity Assessment. To generate a toxicological profile for compound **7** and equipotent derivatives **7f**, **7i**, **7k**, **7l**, **7n**, **7o**, **7q**, and **7r**, we performed a WST-1 cell assay with human HeLa cells. Cell viability was determined after treatment of cells with IL-1β and TNFα and simultaneously with increasing concentrations of the test compounds for 24 h. Stimulation was applied to modulate an inflammatory setting. All tested derivatives showed no or only slightly decreased cell viability at 1 and 10 μM inhibitor concentration (Figure 1). At 100 μM concentration, the derivatives **7k**, **7l**, **7n**, and **7q** as well as the control substance celecoxib decreased cell viability consid-

dx.doi.org/10.1021/jm201687d | J. Med. Chem. 2012, 55, 3792−3803

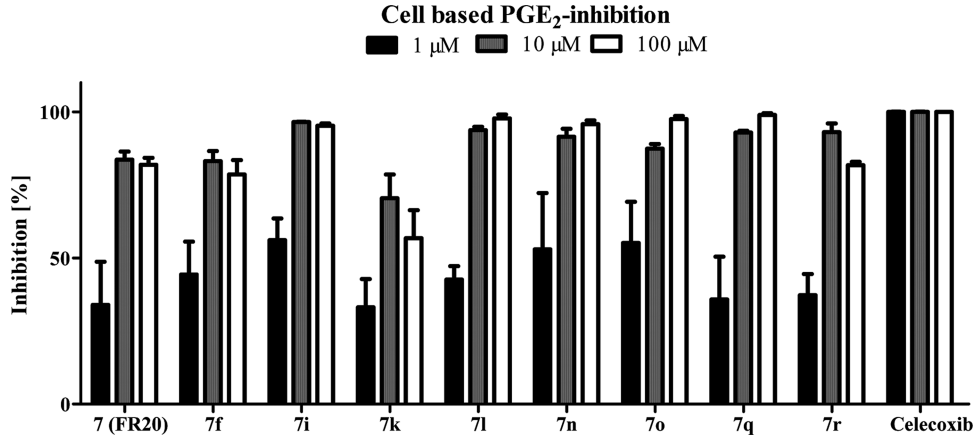

Figure 2. PGE_2 levels were measured with LC/MS-MS technique after incubation of stimulated HeLa cells with different concentrations of test compounds or DMSO. Inhibition is calculated as percent of DMSO control corrected by the background value (unstimulated control) with SEM ($n \geq 3$; **7r**, $n = 2$).

erably. The COX-2 inhibitor celecoxib is already known for its cytotoxic effects in vitro and in vivo and was used to compare the quinazolinone inhibitors with a reference compound used in clinical settings.[25−27]

Cell-Based mPGES-1 Activity Assay. To determine the PGE_2 reducing effect of the compounds on intact HeLa cells, the mPGES-1 inhibitors were simultaneously incubated with a proinflammatory stimulus (IL-1β and TNFα) for 24 h. The production of PGE_2 was determined in the extracellular supernatant and was reduced dose-dependently with all inhibitors (Figure 2). We observed a shift in inhibitory potency in comparison to isolated mPGES-1 enzyme activity of about 28% (**7i**) to 64% (**7n**) at 1 μM compound concentration.

Whole Blood Eicosanoid Profiling. To assemble a preliminary pharmacological profile and to collect first bioavailability data, we screened compound **7** and derivatives **7f**, **7i**, **7k**, **7l**, **7n**, **7o**, **7q**, and **7r** in human whole blood assays. Three different assays were selected to check their influences on (i) COX-1 mediated prostanoid production (mainly TXA_2 and PGD_2), (ii) COX-2 coupled prostanoid synthesis (mainly PGE_2 and $PGF_{2\alpha}$), and (iii) leukotriene/HETE pathways. Table 2 summarizes the remaining levels of each eicosanoid as compared to vehicle treated whole blood. COX-1 mediated prostanoid production was stimulated by platelet clotting of nonheparinized blood. Instead of the instable COX-1 related product TXA_2,[28] the stable metabolite TXB_2 was measured. In this setting, PGD_2 is also slightly up-regulated. No compound had an inhibitory or stimulating effect on the TXB_2 and PGD_2-level up to 10 μM final compound concentration (Table 2A). The selective COX-1 inhibitor SC-560 reduced both TXB_2 and PGD_2 as expected. COX-2 related prostaglandin production was induced by treatment of heparinized whole blood with LPS, which leads to an increase of mainly COX-2/mPGES-1 coupled PGE_2 levels but also to enhanced $PGF_{2\alpha}$ levels. To exclude effects mediated by COX-1, we mixed all samples with 10 μg/mL acetylsalicylic acid (in this concentration a specific COX-1 inhibitor[29]). Except for **7f**, all compounds reduced PGE_2 at 100 μM concentration (Table 2B). Celecoxib also reduced $PGF_{2\alpha}$ levels, while **7f** increased its concentration.

To assess the influence of the compounds on the leukotriene and HETE pathways, we treated heparinized whole blood with calcium-ionophore to activate the 5-lipoxygenase (5-LO)/5-lipoxygenase activating protein (FLAP) complex, leading to an increase of LTA_4 levels[30] (Table 2C−E). Beside LTB_4 (the stable metabolite of LTA_4) also enhanced levels of various hydroxyeicosatetraenoic acids (HETE) were detected after stimulation.[31] The 5-LO-inhibitor zileuton,[32] which was used as control compound, reduced LTB_4 and 5(S)-HETE. Derivative **7f** of the quinazolinone series enhanced both LTB_4 and 5(S)-HETE levels, while the residual production of 5(S)-HETE was reduced by **7i**. All other tested compounds had no influence on LTB_4 and 5(S)-HETE. 12(S)-HETE, 15(S)-HETE, and (±)11-HETE levels were not affected at all at 10 μM final concentration.

DISCUSSION

The primary aim of this study was to generate a library of quinazolinone compounds with different scaffold decorations, to investigate their influence on the mPGES-1 and other enzymes of the eicosanoid pathway, and to identify preliminary structure−activity relationships.

We were able to establish a facile synthesis route for the quinazolinone-based inhibitors of mPGES-1 (Scheme 1). The presented synthesis route is timesaving, needs small amounts of material, and enables chemical modifications of at least three residues around the quinazolinone scaffold. Together with several other compounds purchased from a commercial supplier, we investigated the structure−activity relationship of quinazolinone derivatives of the lead structure **7**. The compound set includes variations at three residue positions with (halogenated) aromatic and heterocyclic groups (like thiophene) as well as aliphatic side chains (Chart 2). It turned out that variations at R_1 in most cases considerably reduced the activity as compared to **7**. Only aromatic residues with an *ortho*-chloro-substitution (**7**, **7f**) were tolerated, which points to the importance of a hydrophobic interaction with the *ortho*-chlorine atom in contrast to unsubstituted phenyl moiety and *ortho*-fluor (**7b** and **7c** with 15% and 30% inhibition at 1 μM). Additionally, *para*-chloro substituents led to decreased activity (**7h**). Moreover, we observed reduced inhibition when R_1 is an aliphatic residue (**7d**, **7e**); larger substituents like phenethyl (**7a**) further impaired activity. Bioisosteric replacement of the *ortho*-substituted phenyl-residue R_1 by a thiophene (**7g**) resulted in a less potent inhibitor than **7**.

With 3-chlorbenzyl moiety in the R_2 position, the disubstitution at R_1 was investigated; **7o** (2-chloro-6-fluoro) and **7p** (2-chloro-6-chloro) exhibit similar inhibitory activity as

dx.doi.org/10.1021/jm201687d | J. Med. Chem. 2012, 55, 3792−3803

Table 2. Human Whole Blood Was Incubated with Quinazolinone Series Compounds[a]

A

Whole Blood COX-1 Assay	TXB_2			PGD_2		
Compound / Concentration	Residual production [%]	SEM [%]	n	Residual production [%]	SEM [%]	n
SC-560 5 μM	0.2	0.1	8	-0.2	1.1	8
7 (FR20) 10 μM	90.0	7.5	5	98.5	8.8	5
7f 10 μM	97.3	5.9	6	96.1	10.8	5
7i 10 μM	89.0	6.1	6	91.7	22.2	6
7k 10 μM	86.4	3.8	5	84.9	14.3	5
7l 10 μM	90.4	4.1	6	86.5	9.5	6
7n 10 μM	86.1	0.9	6	89.0	10.1	6
7o 10 μM	84.4	3.6	6	89.4	15.8	6
7q 10 μM	81.9	3.7	6	128.3	37.6	6

B

Whole Blood COX-2 Assay	PGE_2			PGF_{2a}		
Compound / Concentration	Residual production [%]	SEM [%]	n	Residual production [%]	SEM [%]	n
Celecoxib 5 μM	6.5	1.5	12	7.3	2.6	12
7 (FR20) 100 μM	51.2	2.0	6	94.2	5.9	6
7f 100 μM	173.8	18.0	6	234.0	34.5	6
7i 100 μM	50.0	4.9	6	92.5	10.1	6
7k 100 μM	52.1	7.1	6	92.6	7.0	6
7l 100 μM	37.4	4.5	6	81.3	10.3	6
7n 100 μM	34.2	1.7	6	73.4	7.2	6
7o 100 μM	54.7	1.5	6	97.0	8.3	6
7q 100 μM	53.0	5.8	6	93.8	10.6	6

C

Whole Blood LO/HETE Assay	LTB_4			5(S)-HETE		
Compound / Concentration	Residual production [%]	SEM [%]	n	Residual production [%]	SEM [%]	n
Zileuton 5 μM	20.4	3.1	9	19.1	2.3	9
7 (FR20) 10 μM	83.0	4.5	9	79.0	2.8	9
7f 10 μM	150.8	16.0	9	157.4	20.1	9
7i 10 μM	70.9	6.8	9	67.0	6.2	9
7k 10 μM	71.9	7.7	9	74.8	7.2	9
7l 10 μM	93.7	9.0	9	92.0	9.8	9
7n 10 μM	91.3	3.5	9	88.1	3.5	9
7o 10 μM	94.1	5.0	9	92.1	5.0	9
7q 10 μM	72.7	7.7	9	74.4	7.6	9

D

Whole Blood LO/HETE Assay	12(S)-HETE			15(S)-HETE		
Compound / Concentration	Residual production [%]	SEM [%]	n	Residual production [%]	SEM [%]	n
Zileuton 5 μM	101.3	12.7	9	95.1	7.0	9
7 (FR20) 10 μM	80.0	3.5	9	83.1	5.7	9
7f 10 μM	93.2	10.3	9	93.8	8.2	9
7i 10 μM	85.5	8.2	9	80.0	9.0	9
7k 10 μM	109.5	8.8	9	94.2	10.3	9
7l 10 μM	92.8	10.8	9	90.3	12.2	9
7n 10 μM	82.7	3.7	9	78.3	9.4	9
7o 10 μM	123.0	19.3	9	110.6	10.4	9
7q 10 μM	88.9	18.5	9	83.4	9.9	9

E

Whole Blood LO/HETE Assay	(±)11-HETE		
Compound / Concentration	Residual production [%]	SEM [%]	n
Zileuton 5 μM	93.2	11.3	6
7 (FR20) 10 μM	76.8	6.8	6
7f 10 μM	85.2	9.0	6
7i 10 μM	77.0	11.9	6
7k 10 μM	84.8	17.4	6
7l 10 μM	71.6	12.5	6
7n 10 μM	75.4	12.4	6
7o 10 μM	122.9	10.8	6
7q 10 μM	86.5	18.3	6

[a]Residual production is given in percent of control. Red color indicates a residual production ≤67% (= inhibition), yellow color between 67.1% and 132.9% (= no effect), green color ≥133% (= stimulation) (A) Blood clotting induced mainly COX-1 mediated TXB_2 production, but PGD_2 was also detected. (B) Stimulation of COX-2 and mPGES-1 with LPS upregulated PGE_2 and $PGF_{2\alpha}$-levels. (C−E) Calcium ionophore stimulated whole blood induces LTB_4 production via 5-LO/FLAP but also several HETEs.

7, implicating that a substitution at position 6 of the R_1-phenyl is tolerated. Apparently, the R_2 residue may be exchanged for a smaller substituent without losing potency. Simplification of the [1,1′-biphenyl]-4-ylmethyl- (**7**) to a benzyl-group (**7l**), as well as substitution at the [1,1′-biphenyl]-4-ylmethyl group (**7i**, **7j**) or at the benzyl-group at different positions (**7l**, **7n**) is also tolerated, with no detrimental effect on activity. Variations of the R_3 residue were only possible for some derivatives. A

dx.doi.org/10.1021/jm201687d | J. Med. Chem. 2012, 55, 3792−3803

methyl (**7m**) and a benzyl residue (**7r**) yielded comparable activities, while a replacement with cyclopropyl (**7t**) abolished inhibition. We therefore conclude that residue R_1 is critical for the activity of this class of inhibitors, while R_2 and R_3 play a minor role. These two residues may serve as a starting point for further chemical variations.

In the in vitro single concentration test on isolated human mPGES-1 protein, 13 out of 25 compounds showed an inhibition rate higher than 33%, eight of them with an enhanced potency compared to the lead structure **7** (>66%). These eight inhibitors were used in all further studies. Interestingly, no inhibitor has a lower IC_{50} than **7** (Table 1). To exclude COX-1/COX-2 related side effects, selectivity of the compounds against these two enzymes was tested in a direct inhibitor test. Neither COX-1 nor COX-2 were affected at 1 μM concentration (inhibition ≪33%). Cellular toxicology studies exhibit impaired cell viability at 100 μM inhibitor concentration for four derivatives (Figure 1). All tested compounds reduced the PGE_2 level in a cell-based assay (Figure 2) between 70% (**7k**) and 97% (**7i**) at 10 μM compound concentration. Tests with a 10-fold higher concentration (100 μM) did not enhance the inhibitory effect that was also observed on isolated enzyme. We therefore conclude that there is no major limitation in cell permeability. Whole blood eicosanoid screening revealed a distinct profile for each compound including many fatty acids of the three major arachidonic acid subcascades: the prostanoids, leukotrienes, and HETEs. It has been shown in mPGES-1-deficient mice that PGE_2 synthesis may be redirected to PGD_2, $PGF_{2\alpha}$, and 6-keto-$PGF_{1\alpha}$ (stable metabolite of PGI_2).[33] This mechanism may compensate for a loss of PGE_2 synthesis in nociceptive behavior. We therefore determined the level of other prostanoids and arachidonic acid metabolites. Besides the desired PGE_2 inhibition, no effects on TXB_2 and PGD_2 levels were observed. The role of PGD_2 in pathological conditions seems to be diverse: while exogenous PGD_2 sustains the pyrogenic effects of PGE_2[34] in brain tissue, the metabolite 15d-PGJ_2 is involved in anti-inflammatory responses.[35] Reduction of PGD_2 might therefore delay the resolution of inflammation.[36] $PGF_{2\alpha}$, which is also not affected, mediates allodynia in the spinal cord.[37] In contrast, $PGF_{2\alpha}$ contributes to resolution of inflammation in the late phase of carrageenan-induced pleurisy in rats.[38] In addition, leukotrienes and HETEs play a role in pathological conditions, but their roles are diverse and compound-dependent, suggesting no common mode of action.

While LTB_4 and 5(S)-HETE levels were only slightly affected by the tested quinazolinone substances, 12(S)-HETE, 15(S)-HETE, and (±)11-HETE were not reduced by any derivative. Compound **7f** contrarily enhanced PGE_2, $PGF_{2\alpha}$, LTB_4, and 5(S)-HETE levels, indicating a COX-2/5-LO mediated proinflammatory effect. Nevertheless, whole blood assays revealed that inhibition of mPGES-1 with our compounds is not accompanied by a redirection of COX-derived PGH_2 to other prostanoids and therefore pharmacological inhibition of mPGES-1 seems to be a promising approach for the treatment of pain and inflammation. An approximately 10-fold shift of decreased PGE_2 inhibition potency between activity assays with isolated enzyme and in whole blood was observed for all compounds. A reduced unbound fraction of the compounds due to distribution into cells, membranes, or protein binding may be responsible for this shift but does not automatically limit in vivo efficacy.[39]

CONCLUSIONS

In this study, we discovered that a *ortho*-chloro-substitued phenyl residue at position R_1 and a propyl or benzyl residue at position R_3 of the lead structure **7** promote mPGES-1 inhibition. Structural variations at position R_2 seem to be less influential on mPGES-1 inhibition. A detailed whole blood eicosanoid screening revealed that pharmacological inhibition of mPGES-1 is not accompanied by a redirection of COX derived PGH_2 to other prostanoids.

EXPERIMENTAL SECTION

Chemical Methods. Material and Reagents. Compound **7** and respective derivatives **7a−n** and **7r−x** were purchased from Asinex (Asinex, Moscow, Russia) and exhibit ≥95% purity determined by manufacturer. Compounds **7o−q** were synthesized in-house. The structures of the synthesized compounds were confirmed by ^1H , ^{13}C NMR and mass spectrometry (ESI). The purity of the synthesized compounds was determined by combustion analysis and was found to be >95%. Starting materials and solvents were purchased from Sigma-Aldrich Chemie GmbH (Steinheim, Germany) or Alfa Aesar (Ward Hill, USA) and were reagent grade and used without further purification. For the microwave synthesis, a Biotage Initiator 2.0 (300 W) was used and the products were purified using a Varian 971-FP flash purification system on silica gel with 50 μm particle size. ^1H and ^{13}C NMR spectra were measured in DMSO-d_6 or MeOD on a Bruker AV 250 (250 MHz for ^1H NMR and 63 MHz for the ^{13}C NMR). Chemical shifts are reported in parts per million (ppm) using tetramethylsilane (TMS) as internal standard. Mass spectra were obtained on an Electrospray-Ionization Fisons (VG Platform II) spectrometer measuring in the positive- or negative-ion mode (ESI-MS system). Combustion analysis was performed by the micro-analytical laboratory of the Institute of Organic Chemistry and Chemical Biology, Goethe University Frankfurt, on an Elementar Vario Micro Tube CHNO rapid elemental analyzer.

Synthesis. The compounds were synthesized in three steps (Scheme 1) involving the condensation of 5-iodoanthranilic acid with butyric acid followed by dehydration to form the intermediate benzoxazinone. Successive addition of 3-chlorbenzylamine provides 2,3-disubstituted-6-iodo-3*H*-quinazolin-4-one; these reactions were carried out under microwave conditions.[40] The third step comprises a related Goldberg reaction,[41] a copper-catalyzed *N*-arylation of amides with a heteroaryl iodide. The reaction is mediated by copper iodide, *N*,*N*′-dimethylethylenediamine, and K_3PO_4.

Synthesis of 3-(3-Chlorobenzyl)-6-iodo-2-propylquinazolin-4(3H)-one. To a conical-bottomed microwave vial, a solution of 5-iodoanthranilic acid (0.500 g, 1.901 mmol, 1 equiv), butyric acid (0.167 g, 1.901 mmol, 1 equiv), and triphenyl phosphite (0.639 g, 2.091 mmol, 1.1 equiv) in 2 mL of anhydrous pyridine was added. The mixture was irradiated in a sealed microwave vial for 10 min at 150 °C. After cooling, 3-chlorbenzylamine (0.269 g, 1.901 mmol, 1 equiv) was added and irradiated for 5 min at 230 °C. The solvent was removed, and the residue was resolved in ethyl acetate, washed with saturated $NaHCO_3$ (2 × 10 mL), 10% HCl (2 × 10 mL), and dried over $MgSO_4$. The solvent was removed under reduced pressure, and the crude product was purified by column chromatography on silica gel with hexane−ethyl acetate (50:50, v/v), obtaining 100 mg (12% yield) of an off-white solid.

^1H NMR (MeOD): δ 8.60 (br, 1H), 8.19 (dd, J = 3.4, 8.6 Hz, 1H), 7.48 (d, J = 8.6 Hz, 1H), 7.33 (m, 3H), 5.46 (s, 2H), 2.87 (t, J = 7.8 Hz, 2H), 1.73 (q, J = 7.5 Hz, 2H), 1.00 (t, J = 7.3 Hz, 3H).

MS (ESI, 70 eV) m/z (%): 439.2 (100%).

*Synthesis of 2-Chloro-N-(3-(3-chlorobenzyl)-4-oxo-2-propyl-3,4-dihydroquinazolin-6-yl)-6-fluorobenzamide (**7o**).* A round-bottomed flask was charged with CuI (1 mg, 0.005 mmol, 0.01 equiv), 2-chloro-6-fluorobenzamide (0.114 g, 0.657 mmol, 1.2 equiv), and K_3PO_4 (0.232 g, 1.094 mmol, 2 equiv), evacuated, and backfilled with argon. *N*,*N*′-Dimethylethylenediamine (4 mg, 0.055 mmol, 0.1 equiv), 3-(3-chlorobenzyl)-6-iodo-2-propylquinazolin-4(3*H*)-one (0.240 g, 0.547

dx.doi.org/10.1021/jm201687d | J. Med. Chem. 2012, 55, 3792−3803

mmol, 1 equiv), and tetrahydrofuran (10 mL) were added under argon. The reaction mixture was stirred at 110 °C for 23 h. The resulting pale-brown suspension was cooled down and filtered through a 1 cm pad of silica gel eluting with 20 mL of ethyl acetate. The filtrate was concentrated, and the residue was purified by column chromatography on silica gel with hexane−ethyl acetate (50:50, v/v) provided 189 mg (71% yield) as an off-white solid.

^{1}H NMR (DMSO-d_6): δ 11.19 (br, 1H), 8.68 (d, J = 2.4, 1H), 8.05 (dd, J = 2.4, 8.8 Hz, 1H), 7.73 (d, J = 8.7 Hz, 1H), 7.79−7.43 (m, 6H), 7.17 (d, J = 5.4 Hz, 1H), 5.43 (s, 2H), 2.76 (t, J = 14.8 Hz, 2H), 1.77 (q, J = 7.3 Hz, 2H), 0.96 (t, J = 7.3 Hz, 3H).

^{13}C NMR (DMSO-d_6): δ 163.5, 161.7, 160.5, 156.8, 156.1, 143.9, 139.7, 136.6, 133.7, 132.0, 130.9, 127.9, 126.6, 125.8, 124.9, 120.3, 115.7, 114.8, 45.2, 35.8, 19.8, 13.6.

MS (ESI, 70 eV) m/z (%): 484.5 (100%).

Anal. Calcd for $C_{25}H_{20}Cl_2FN_3O_2$: C, 61.99, H, 4.16, N, 8.68. Found: C, 61.95, H, 4.12, N, 8.64.

*Synthesis of 2,6-Dichloro-N-(3-(3-chlorobenzyl)-4-oxo-2-propyl-3,4-dihydroquinazolin-6-yl)benzamide (**7p**).* A round-bottomed flask was charged with CuI (3 mg, 0.015 mmol, 0.05 equiv), 2,6-dichlorobenzamide (0.09 g, 0.478 mmol, 1.5 equiv), and K_3PO_4 (0.132 g, 0.638 mmol, 2 equiv), evacuated, and backfilled with argon. *N*,*N*′-Dimethylethylenediamine (3 mg, 0.031 mmol, 0.1 equiv), 3-(3-chlorobenzyl)-6-iodo-2-propylquinazolin-4(3*H*)-one (0.140 g, 0.319 mmol, 1 equiv), and THF (10 mL) were added under argon. The reaction mixture was stirred at 110 °C for 23 h. The resulting pale-brown suspension was cooled down and filtered through a 1 cm pad of silica gel eluting with 20 mL of ethyl acetate. The filtrate was concentrated, and the residue was recrystallized from EtOH/water, obtaining 80 mg (50% yield) as a white solid.

^{1}H NMR (DMSO-d_6): δ 11.18 (br, 1H), 8.70 (d, J = 3.3 Hz, 1H), 8.05 (dd, J = 3.3, 9.2 Hz, 1H), 7.76−7.21 (m, 7H), 7.15 (m, 1H), 5.48 (s, 2H), 2.77 (t, J = 8.3 Hz, 2H), 1.78 (q, J = 9.6 Hz, 2H), 0.95 (t, J = 8.2 Hz, 3H).

^{13}C NMR (DMSO-d_6): 162.3, 161.3, 155.9, 143.5, 142.6, 139.4, 136.9, 136.0, 133.6, 131.9, 131.1, 128.2, 126.4, 125.3, 119.9, 115.4, 45.4, 35.7, 19.6, 13.3.

MS (ESI, 70 eV) m/z (%): 500.3 (100%).

Anal. Calcd for $C_{25}H_{20}Cl_3N_3O_2$: C, 59.96, H, 4.03, N, 8.39. Found: C, 60.19, H, 4.21, N, 8.36.

*Synthesis of N-(3-(3-Chlorobenzyl)-4-oxo-2-propyl-3,4-dihydroquinazolin-6-yl)-2-methylbenzamide (**7q**).* A round-bottomed flask was charged with CuI (43 mg, 0.228 mmol, 0.2 equiv), 2-methylbenzamide (0.185 g, 1.368 mmol, 1.2 equiv), and K_3PO_4 (0.484 g, 2.280 mmol, 2 equiv), evacuated, and backfilled with argon. *N*,*N*′-Dimethylethylenediamine (40 mg, 0.456 mmol, 0.4 equiv), 3-(3-chlorobenzyl)-6-iodo-2-propylquinazolin-4(3*H*)-one (0.5 g, 1.140 mmol, 1 equiv), and THF (10 mL) were added under argon. The reaction mixture was stirred at 110 °C for 23 h. The resulting pale-brown suspension was cooled down and filtered through a 1 cm pad of silica gel eluting with 20 mL of ethyl acetate. The filtrate was concentrated, and the residue was purified by flash chromatography on silica gel (hexane−ethyl acetate, 0→ 80% ethyl acetate, 4%/min) provided 179 mg (35% yield) as an off-white solid.

^{1}H NMR (DMSO-d_6): δ 10.69 (br, 1H), 8.74 (d, J = 2.1 Hz, 1H), 8.13 (dd, J = 2.3, 8.8 Hz, 1H), 7.70 (d, J = 8.8 Hz, 1H), 7.56 (d, J = 7.0 Hz, 1H), 7.49−7.33 (m, 6H), 7.07 (m, 1H), 5.45 (s, 2H), 2.76 (t, J = 7.4 Hz, 2H), 2.48 (s, 3H), 1.76 (q, J = 7.3 Hz, 2H), 0.96 (t, J = 7.3 Hz, 3H).

^{13}C NMR (DMSO-d_6): δ 168.2, 161.4, 155.8, 143.0, 139.4, 136.9, 135.6, 133.4, 130.7, 129.9, 129.1, 126.9, 125.8, 124.7, 120.3, 115.6, 45.3, 36.0, 19.4, 19.1, 13.6.

MS (ESI, 70 eV) m/z (%): 446.5 (100%).

Anal. Calcd for $C_{26}H_{24}ClN_3O_2$: C, 70.03, H, 5.42, N, 9.42. Found: C, 69.94, H, 5.33, N, 9.21.

Cell Biological Methods. Cells and Reagents. HeLa (human cervix carcinoma) and NIH-3T3 (Swiss mouse fibroblast) cells were purchased from Deutsche Sammlung für Mikroorganismen and Zellkulturen (DSMZ, Braunschweig, Germany). RAW 264.7 (mouse macrophage) cells were purchased from American Type Culture Collection (ATCC, Manassas, USA). HeLa were incubated in RPMI medium 1640 containing high glucose, L-glutamine, and 25 mM HEPES, NIH in Dulbecco's MEM containing 4.5 g/L glucose, and pyruvate and RAW in RPMI medium 1640, containing high glucose, GlutaMAX. All media contain 10% fetal calf serum (FCS), 100 units/mL penicillin G, and 100 μg/mL streptomycin, which were purchased from Invitrogen (Darmstadt, Germany). Cells were cultured at 37 °C in an atmosphere containing 5% CO_2. Recombinant human IL-1 β (IL-1β) and recombinant human tumor necrosis factor α (TNFα) were purchased from PeproTech (London, UK).

mPGES-1 Activity Assay. To investigate the inhibitory activity of the quinazolinone derived compounds on the mPGES-1 enzymes in vitro, the microsomal fraction of human HeLa, murine RAW, and murine NIH cells were prepared. Approximately 3 × 10^6 cells were incubated for 24 h at 37 °C in medium containing 10% FCS. The medium was removed, and HeLa/NIH cells were stimulated with IL-1β (1 ng/mL) + TNFα (5 ng/mL) for 16 h, RAW cells were stimulated with 10 mg/mL LPS for 16 h. Cells were scraped in 2 mL of phosphate buffered saline (PBS) and centrifuged at 5000 rpm for 2 min at 4 °C. Cell pellets were frozen in liquid nitrogen. After thawing the cells, they were resuspended in 800 μL of potassium phosphate buffer (Kpi buffer, 0.1 M, pH 7.4), containing 1× complete protease inhibitor cocktail (Roche Diagnostics, Mannheim, Germany), sucrose (0.25 M), and reduced glutathione (GSH, 1 mM). After sonification and centrifugation at 45000 rpm for 2 h or 53000 rpm for 1 h at 4 °C, the microsomal fraction (pellet) was stored at −80 °C. The pellet was resuspended in 100 μL Kpi buffer (0.1 M, pH 7.4) containing 1× Roche Complete and reduced GSH (2.5 mM). To homogenize the solution, a sonification step was applied and total protein content was measured using the Bradford method.[42] Activity of all quinazolinone derivates was measured at 1 μM final concentration and compared to the lead compound. The mPGES-1 activity assay was performed on the basis of Thoren et al.[43] Briefly, 0.15 mg/mL of human HeLa derived or murine NIH derived protein or 0.3 mg/mL of murine RAW derived protein was incubated with each compound for 30 min on ice. The reaction was initiated with 20 μM PGH_2 (Larodan, Malmö, Sweden) and terminated after 1 min by adding a stop solution containing 40 mM iron chloride ($FeCl_2$) and 80 mM citric acid. For the solid phase extraction procedure, 100 μL of reaction solution was mixed for 3 min with 700 μL of ultrapure water, 100 μL of 0.15 M EDTA, 20 μL of MeOH, and 20 μL of internal standard (25 ng/mL PGE_2-d_4, 50 ng/mL PGD_2-d_4), all from Cayman Chemical Company (Ann Arbor, USA), centrifuged at 1200 rpm for 3 min, and passed through a 30 mg of Bond Elut NEXUS 96 round-well plate (Agilent Technologies GmbH, Böblingen, Germany) preconditioned with 1 mL of MeOH, followed by 1 mL of ultrapure water. The cartridge was washed with 1 mL of 30% MeOH. Prostaglandins were eluted with 1 mL of hexane−ethylacetate−isopropranol (30:65:5, v/v/v). After evaporating the solvent under nitrogen atmosphere, the residue was reconstituted in 100 μL of acetonitrile−H_2O−formic acid (20:80:0.0025 v/v/v). Samples were measured by LC-MS/MS technique (LC unit: Agilent 1200 series, Agilent Technologies GmbH, Böblingen, Germany. MS/MS unit: AB SCIEX QTRAP 5500, Applied Biosystems, Foster City, USA) as described previously.[44] Compounds with improved inhibitory effect as compared to the lead structure were used for further experiments. For IC_{50} calculation, the mPGES-1 assay was performed with increasing compound concentrations. The IC_{50} was calculated using GraphPad Prism 5 software (GraphPad Software, Inc., San Diego, CA 92130 USA) by fitting the four parameter logistic curve. With 95% probability, the estimated IC_{50} is in the range of the given confidence interval.

COX-Inhibitor Screening Assay. To distinguish between mPGES-1 and COX-1 or COX-2 derived inhibition of PGE_2 production, direct inhibition of the COX-1 (ovine) and COX-2 (human recombinant) enzyme was measured using a COX inhibitor screening assay kit (Cayman Chemicals, Ann Arbor, MI, USA), according to the manufacturer's protocol. SC-560, a selective COX-1 inhibitor, and celecoxib, a selective COX-2 inhibitor, were used as positive controls. The COX assay is based on the determination of PGE_2, PGD_2, and

$PGF_{2\alpha}$ amounts produced by $SnCl_2$ reduction of COX-derived PGH_2. Then 100 μL of reaction solution was diluted with 200 μL of MeOH. Finally, 70 μL of diluted reaction solution was mixed for 3 min with 700 μL of ultrapure water, 100 μL of 0.15 M EDTA, 20 μL of MeOH, and 20 μL of internal standard (25 ng/mL PGE_2-d_4, 25 ng/mL PGD_2-d_4, 25 ng/mL TXB_2-d_4, 50 ng/mL $PGF_{2\alpha}$-d_4, 37.5 ng/mL 6-keto-$PGF_{1\alpha}$-d_4). The amount of prostaglandins was quantified by LC-MS/MS analysis after solid phase extraction as described above (see mPGES-1 activity assay).

WST-1 Cell Viability Assay. The water-soluble tetrazolium-1 salt (Roche Diagnostics, Mannheim, Germany) was used to determine the cell viability after treatment of cells with the compounds. HeLa cells were seeded at a density of 3×10^3 cells in 100 μL of culture medium containing 10% FCS into 96-well microplates and incubated for 24 h at 37 °C. Medium was removed, and HeLa cells were stimulated with IL-1β (1 ng/mL) + TNFα (5 ng/mL) and simultaneously treated with increasing concentrations of the compounds (1, 10, and 100 μM) or DMSO. After 24 h, 10 μL of WST-1 reagent was added to each well and the cells were incubated for further 90−150 min. The formation of the dye was measured at 450 nm against a reference wavelength of 620 nm using a 96-well spectrophotometric plate reader (SpectraFluor Plus, Tecan, Crailsheim, Germany).

Cell-Based mPGES-1 Activity Assay. first, 2×10^4 HeLa cells were incubated in 24-well microplates for 24 h at 37 °C. Then the medium was replaced with fresh medium containing 1 ng/mL IL-1β + 5 ng/mL TNFα (stimulated control) or an equal amount of PBS (unstimulated control) and test compound (1, 10, or 100 μM) or DMSO. After incubation for 24 h at 37 °C, cell supernatant was collected. Then 400−500 μL of supernatant was mixed with 400 μL of 45 mM H_3PO_4, 100 μL of 0.15 M EDTA, 20 μL of MeOH, and 20 μL of internal standard (25 ng/mL PGE_2-d_4, 25 ng/mL PGD_2-d_4, 25 ng/mL TXB_2-d_4, 50 ng/mL $PGF_{2\alpha}$-d_4, 37.5 ng/mL 6-keto-$PGF_{1\alpha}$-d_4). The amount of prostaglandins was quantified by LC-MS/MS analysis after solid phase extraction as described above (see mPGES-1 activity assay).

Whole Blood Eicosanoid Screening. To determine possible effects of quinazolinone derivatives on different eicosanoids levels in human whole blood, a eicosanoid profile was created for each compound. Therefore, three different experimental settings were used to stimulate the production of eicosanoid synthesis.

A stimulating effect of a compound was assumed when the relative level of an eicosanoid exceeded +33% compared to control, an inhibitory effect when levels were reduced by −33% or more, as compared to control.

Whole Blood COX-1 Assay. Because TXA_2 is the major product of the COX-1/thromboxane-A synthase-pathway (which is activated during blood clotting), this setting was used to investigate the effect of mPGES-1 inhibitors on these two enzymes. Human venous whole blood was collected in neutral monovettes without any additives (SARSTEDT AG & Co, Nümbrecht, Germany) from healthy donors who had not taken any NSAIDs for at least one week. Then 500 μL of blood per sample was directly mixed with rising concentrations of test compounds. Negative controls were immediately chilled on ice to minimize thrombocyte aggregation. All other samples were incubated at 37 °C for 1 h, and blood was allowed to clot.

Samples were chilled on ice for 5 min, and plasma was extracted by centrifugation at 4 °C with 2000 rpm for 20 min. Plasma samples were stored at −80 °C. For the extraction procedure, plasma was mixed for 3 min with 600 μL of 45 mM H_3PO_4, 100 μL of 0.15 M EDTA, 10 μL of 2 mg/mL butylated hydroxytoluene, 20 μL of MeOH, and 20 μL of internal standard (25 ng/mL PGE_2-d_4, 25 ng/mL PGD_2-d_4, 25 ng/mL TXB_2-d_4, 50 ng/mL $PGF_{2\alpha}$-d_4, 37.5 ng/mL 6-keto-$PGF_{1\alpha}$-d_4).

TXB_2 (instead of the instable TXA_2) was measured together with PGE_2, PGD_2, 6-keto-$PGF_{1\alpha}$, and PGF_{2a} after solid phase extraction as described above (see mPGES-1 activity assay).

Whole Blood COX-2 Assay. The mPGES-1 expression is mainly coupled to COX-2 and therefore many proinflammatory stimuli, activating the COX-2, also upregulate the protein level of mPGES-1. For the COX-2 assay, blood was collected in NH_4−heparin containing monovettes (SARSTEDT AG & Co, Nümbrecht, Germany) which prevent blood clotting. Then 500 μL of heparinized blood was mixed with test compounds in DMSO. Finally, 10 μg/mL acetylsalicylic acid was added to inhibit COX-1. After 15 min incubation at 37 °C, 500 μg/mL (10 μg/mL final concentration) lipopolysaccharide (LPS) in 10 μL autologous plasma was added to stimulate COX-2/mPGES-1. After 24 h incubation time at 37 °C, samples were chilled on ice for 5 min and plasma was collected and prostaglandins extracted and measured by LC-MS/MS (see Whole Blood COX-1 Assay).

Whole Blood Leukotriene/HETE Assay. To assess the influence of quinazolinone derivatives on different enzymes in the leukotriene and HETE pathway, 500 μL of human heparinized whole blood was mixed with test compounds and incubated for 15 min at 37 °C. Afterward, the whole blood was stimulated with 20 μM calcium ionophore (A23187) in autologous plasma for a further 15 min at 37 °C. Blood samples were chilled on ice for 5 min, plasma collected (centrifugation at 4 °C with 2000 rpm for 20 min), and leukotrienes and HETEs extracted by liquid−liquid extraction. Therefore, plasma was mixed with 20 μL of EtOH and 20 μL of internal standard containing 25 ng/mL LTB_4-d_4, 25 ng/mL 5(S)-HETE-d_8, 25 ng/mL 12(S)-HETE-d_8, 25 ng/mL 15(S)-HETE-d_8, and 25 ng/mL 20-HETE-d_6. Then 600 μL of ethyl acetate was added and samples were mixed and centrifuged at 13000 rpm for 3 min. The organic upper phase was extracted. Extraction of leukotrienes and HETEs was repeated once. Solvent was evaporated under nitrogen atmosphere, and the residue was reconstituted in 50 μL of MeOH−H_2O (50:50 v/v). LTB_4, 5(S)-HETE, 12(S)-HETE, 15(S)-HETE, and 20-HETE were analyzed by LC-MS/MS technique on a AB SCIEX QTRAP 5500 (Applied Biosystems, Foster City, CA, USA) operating in multiple reaction monitoring (MRM).[45] Chromatographic separation was performed on a Gemini-NX 5u C18 110A column (150 mm × 2 mm inner diameter, 5 μm particle size, Phenomenex, Aschaffenburg, Germany).

■ ASSOCIATED CONTENT

Ⓢ Supporting Information

IC_{50} dose−response curve of compound **7**. This material is available free of charge via the Internet at http://pubs.acs.org.

■ AUTHOR INFORMATION

Corresponding Author

*Phone: +49 69 6301 6086. Fax: +49 69 6301 7636. E-mail: Roersch@em.uni-frankfurt.de.

Notes

The authors declare no competing financial interest.

■ ACKNOWLEDGMENTS

This research was supported by Merz GmbH & Co. KGaA, the LOEWE Lipid Signaling Forschungszentrum Frankfurt (LiFF), the Oncogenic Signaling Frankurt (OSF), the European Graduate School "Roles of Eicosanoids in Biology and Medicine" (DFG GRK 757/1), the DAAD/Fundación Obra Social "la Caixa", and the Fonds der Chemischen Industrie.

■ ABBREVIATIONS USED

5-LO, 5-lipoxygenase; COX, cyclooxygenase; HETE, hydroxyeicosatetranoid acid; IC_{50}, half-maximal inhibitory concentration; LC-MS/MS, liquid chromatography with combined tandem mass spectrometry; LPS, lipopolysaccharide; LTB_4, leukotrien B_4; mPGES-1, microsomal prostaglandin E synthase 1; NSAIDs, nonsteroidal anti-inflammatory drugs; PGE_2, prostaglandin E_2; SAR, structure−activity relationship

■ REFERENCES

(1) Murakami, M.; Naraba, H.; Tanioka, T.; Semmyo, N.; Nakatani, Y.; Kojima, F.; Ikeda, T.; Fueki, M.; Ueno, A.; Oh, S.; Kudo, I. Regulation of prostaglandin E2 biosynthesis by inducible membrane-

associated prostaglandin E2 synthase that acts in concert with cyclooxygenase-2. *J. Biol. Chem.* **2000**, *275*, 32783−32792.
(2) Kamei, D.; Yamakawa, K.; Takegoshi, Y.; Mikami-Nakanishi, M.; Nakatani, Y.; Oh-Ishi, S.; Yasui, H.; Azuma, Y.; Hirasawa, N.; Ohuchi, K.; Kawaguchi, H.; Ishikawa, Y.; Ishii, T.; Uematsu, S.; Akira, S.; Murakami, M.; Kudo, I. Reduced pain hypersensitivity and inflammation in mice lacking microsomal prostaglandin e synthase-1. *J. Biol. Chem.* **2004**, *279*, 33684−33695.
(3) Trebino, C. E.; Stock, J. L.; Gibbons, C. P.; Naiman, B. M.; Wachtmann, T. S.; Umland, J. P.; Pandher, K.; Lapointe, J. M.; Saha, S.; Roach, M. L.; Carter, D.; Thomas, N. A.; Durtschi, B. A.; McNeish, J. D.; Hambor, J. E.; Jakobsson, P. J.; Carty, T. J.; Perez, J. R.; Audoly, L. P. Impaired inflammatory and pain responses in mice lacking an inducible prostaglandin E synthase. *Proc. Natl. Acad. Sci. U.S.A.* **2003**, *100*, 9044−9049.
(4) Engblom, D.; Saha, S.; Engstrom, L.; Westman, M.; Audoly, L. P.; Jakobsson, P. J.; Blomqvist, A. Microsomal prostaglandin E synthase-1 is the central switch during immune-induced pyresis. *Nature Neurosci.* **2003**, *6*, 1137−1138.
(5) Wang, D.; Dubois, R. N. Eicosanoids and cancer. *Nature Rev. Cancer* **2010**, *10*, 181−193.
(6) Korotkova, M.; Jakobsson, P. J. Microsomal prostaglandin E synthase-1 in rheumatic diseases. *Front. Pharmacol.* **2011**, 1.
(7) Abdel-Tawab, M.; Zettl, H.; Schubert-Zsilavecz, M. Nonsteroidal anti-inflammatory drugs: a critical review on current concepts applied to reduce gastrointestinal toxicity. *Curr. Med. Chem.* **2009**, *16*, 2042−2063.
(8) Timmers, L.; Pasterkamp, G.; de Kleijn, D. P. Microsomal prostaglandin E2 synthase: a safer target than cyclooxygenases? *Mol. Interventions* **2007**, *7* (195−199), 180.
(9) Takemiya, T. Prostaglandin E(2) produced by microsomal prostaglandin E synthase-1 regulates the onset and the maintenance of wakefulness. *Neurochem. Int.* **2011**, *59*, 922−924.
(10) Radmark, O.; Samuelsson, B. Microsomal prostaglandin E synthase-1 and 5-lipoxygenase: potential drug targets in cancer. *J. Intern. Med.* **2010**, *268*, 5−14.
(11) Scholich, K.; Geisslinger, G. Is mPGES-1 a promising target for pain therapy? *Trends Pharmacol. Sci.* **2006**, *27*, 399−401.
(12) Rahme, E.; Roussy, J. P.; Lafrance, J. P.; Nedjar, H.; Morin, S. Use of nonsteroidal antiinflammatory drugs: is there a change in patient risk profile after withdrawal of rofecoxib? *J. Rheumatol.* **2011**, *38*, 195−202.
(13) Tiliakos, A. M.; Conn, D. L. Aspirin: antiinflammatory drug of choice in 2011? *J. Rheumatol.* **2011**, *38*, 185−187.
(14) Chang, H. H.; Meuillet, E. J. Identification and development of mPGES-1 inhibitors: where we are at? *Future Med. Chem.* **2011**, *3*, 1909−1934.
(15) Guerrero, M. D.; Aquino, M.; Bruno, I.; Riccio, R.; Terencio, M. C.; Paya, M. Anti-inflammatory and analgesic activity of a novel inhibitor of microsomal prostaglandin E synthase-1 expression. *Eur. J. Pharmacol.* **2009**, *620*, 112−119.
(16) Bruno, A.; Di Francesco, L.; Coletta, I.; Mangano, G.; Alisi, M. A.; Polenzani, L.; Milanese, C.; Anzellotti, P.; Ricciotti, E.; Dovizio, M.; Di Francesco, A.; Tacconelli, S.; Capone, M. L.; Patrignani, P. Effects of AF3442 [*N*-(9-ethyl-9*H*-carbazol-3-yl)-2-(trifluoromethyl)-benzamide], a novel inhibitor of human microsomal prostaglandin E synthase-1, on prostanoid biosynthesis in human monocytes in vitro. *Biochem. Pharmacol.* **2010**, *79*, 974−981.
(17) Mbalaviele, G.; Pauley, A. M.; Shaffer, A. F.; Zweifel, B. S.; Mathialagan, S.; Mnich, S. J.; Nemirovskiy, O. V.; Carter, J.; Gierse, J. K.; Wang, J. L.; Vazquez, M. L.; Moore, W. M.; Masferrer, J. L. Distinction of microsomal prostaglandin E synthase-1 (mPGES-1) inhibition from cyclooxygenase-2 inhibition in cells using a novel, selective mPGES-1 inhibitor. *Biochem. Pharmacol.* **2010**, *79*, 1445−1454.
(18) Xu, D.; Rowland, S. E.; Clark, P.; Giroux, A.; Cote, B.; Guiral, S.; Salem, M.; Ducharme, Y.; Friesen, R. W.; Methot, N.; Mancini, J.; Audoly, L.; Riendeau, D. MF63 [2-(6-chloro-1*H*-phenanthro[9,10-*d*]imidazol-2-yl)-isophthalonitrile], a selective microsomal prostaglandin E synthase-1 inhibitor, relieves pyresis and pain in preclinical models of inflammation. *J. Pharmacol. Exp. Ther.* **2008**, *326*, 754−763.
(19) Greiner, C.; Zettl, H.; Koeberle, A.; Pergola, C.; Northoff, H.; Schubert-Zsilavecz, M.; Werz, O. Identification of 2-mercaptohexanoic acids as dual inhibitors of 5-lipoxygenase and microsomal prostaglandin E(2) synthase-1. *Bioorg. Med. Chem.* **2011**, *19*, 3394−3401.
(20) Hieke, M.; Greiner, C.; Dittrich, M.; Reisen, F.; Schneider, G.; Schubert-Zsilavecz, M.; Werz, O. Discovery and Biological Evaluation of a Novel Class of Dual Microsomal Prostaglandin E(2) Synthase-1/5-lipoxygenase Inhibitors Based on 2-[(4,6-Diphenethoxypyrimidin-2-yl)thio]hexanoic Acid. *J. Med. Chem.* **2011**, *54*, 4490−4507.
(21) Koeberle, A.; Rossi, A.; Zettl, H.; Pergola, C.; Dehm, F.; Bauer, J.; Greiner, C.; Reckel, S.; Hoernig, C.; Northoff, H.; Bernhard, F.; Dotsch, V.; Sautebin, L.; Schubert-Zsilavecz, M.; Werz, O. The molecular pharmacology and in vivo activity of 2-(4-chloro-6-(2,3-dimethylphenylamino)pyrimidin-2-ylthio)octanoic acid (YS121), a dual inhibitor of microsomal prostaglandin E2 synthase-1 and 5-lipoxygenase. *J. Pharmacol. Exp. Ther.* **2010**, *332*, 840−848.
(22) Revermann, M.; Mieth, A.; Popescu, L.; Paulke, A.; Wurglics, M.; Pellowska, M.; Fischer, A.; Steri, R.; Maier, T.; Schermuly, R.; Geisslinger, G.; Schubert-Zsilavecz, M.; Brandes, R.; Steinhilber, D. A pirinixic acid derivative (LP105) inhibits murine 5-lipoxygenase activity and attenuates vascular remodelling in a murine model of aortic aneurysm. *Br. J. Pharmacol.* **2011**, *163*, 1721−1732.
(23) Bauer, J.; Koeberle, A.; Dehm, F.; Pollastro, F.; Appendino, G.; Northoff, H.; Rossi, A.; Sautebin, L.; Werz, O. Arzanol, a prenylated heterodimeric phloroglucinyl pyrone, inhibits eicosanoid biosynthesis and exhibits anti-inflammatory efficacy in vivo. *Biochem. Pharmacol.* **2011**, *81*, 259−268.
(24) Rörsch, F.; Wobst, I.; Zettl, H.; Schubert-Zsilavecz, M.; Grosch, S.; Geisslinger, G.; Schneider, G.; Proschak, E. Nonacidic inhibitors of human microsomal prostaglandin synthase 1 (mPGES 1) identified by a multistep virtual screening protocol. *J. Med. Chem.* **2010**, *53*, 911−915.
(25) Backhus, L. M.; Petasis, N. A.; Uddin, J.; Schönthal, A. H.; Bart, R. D.; Lin, Y.; Starnes, V. A.; Bremner, R. M. Dimethyl celecoxib as a novel non-cyclooxygenase 2 therapy in the treatment of non-small cell lung cancer. *J. Thorac. Cardiovasc. Surg.* **2005**, *130*, 1406−1412.
(26) Grösch, S.; Maier, T. J.; Schiffmann, S.; Geisslinger, G. Cyclooxygenase-2 (COX-2)-independent anticarcinogenic effects of selective COX-2 inhibitors. *J. Natl. Cancer Inst.* **2006**, *98*, 736−747.
(27) Khan, Z.; Khan, N.; Tiwari, R. P.; Sah, N. K.; Prasad, G. B.; Bisen, P. S. Biology of Cox-2: an application in cancer therapeutics. *Curr. Drug Targets* **2011**, *12*, 1082−1093.
(28) Casetta, B.; Vecchione, G.; Tomaiuolo, M.; Margaglione, M.; Grandone, E. Setting up a 2D-LC/MS/MS method for the rapid quantitation of the prostanoid metabolites 6-oxo-PGF(1alpha) and TXB2 as markers for hemostasis assessment. *J. Mass. Spectrom.* **2009**, *44*, 346−352.
(29) Warner, T. D.; Giuliano, F.; Vojnovic, I.; Bukasa, A.; Mitchell, J. A.; Vane, J. R. Nonsteroid drug selectivities for cyclo-oxygenase-1 rather than cyclo-oxygenase-2 are associated with human gastrointestinal toxicity: a full in vitro analysis. *Proc. Natl. Acad. Sci. U.S.A.* **1999**, *96*, 7563−7568.
(30) Samuelsson, B.; Dahlen, S. E.; Lindgren, J. A.; Rouzer, C. A.; Serhan, C. N. Leukotrienes and lipoxins: structures, biosynthesis, and biological effects. *Science* **1987**, *237*, 1171−1176.
(31) Taylor, S. M.; Liggitt, H. D.; Laegreid, W. W.; Silflow, R.; Leid, R. W. Arachidonic acid metabolism in bovine alveolar macrophages. Effect of calcium ionophore on lipoxygenase products. *Inflammation* **1986**, *10*, 157−165.
(32) Berger, W.; De Chandt, M. T.; Cairns, C. B. Zileuton: clinical implications of 5-lipoxygenase inhibition in severe airway disease. *Int. J. Clin. Pract.* **2007**, *61*, 663−676.
(33) Brenneis, C.; Coste, O.; Schmidt, R.; Angioni, C.; Popp, L.; Nusing, R. M.; Becker, W.; Scholich, K.; Geisslinger, G. Consequences of altered eicosanoid patterns for nociceptive processing in mPGES-1-deficient mice. *J. Cell. Mol. Med.* **2008**, *12*, 639−648.

(34) Gao, W.; Schmidtko, A.; Lu, R.; Brenneis, C.; Angioni, C.; Schmidt, R.; Geisslinger, G. Prostaglandin D(2) sustains the pyrogenic effect of prostaglandin E(2). *Eur. J. Pharmacol.* **2009**, *608*, 28−31.
(35) Scher, J. U.; Pillinger, M. H. The anti-inflammatory effects of prostaglandins. *J. Invest. Med.* **2009**, *57*, 703−708.
(36) Gilroy, D. W.; Colville-Nash, P. R.; Willis, D.; Chivers, J.; Paul-Clark, M. J.; Willoughby, D. A. Inducible cyclooxygenase may have anti-inflammatory properties. *Nature Med.* **1999**, *5*, 698−701.
(37) Muratani, T.; Nishizawa, M.; Matsumura, S.; Mabuchi, T.; Abe, K.; Shimamoto, K.; Minami, T.; Ito, S. Functional characterization of prostaglandin F2alpha receptor in the spinal cord for tactile pain (allodynia). *J. Neurochem.* **2003**, *86*, 374−382.
(38) Colville-Nash, P. R.; Gilroy, D. W.; Willis, D.; Paul-Clark, M. J.; Moore, A. R.; Willoughby, D. A. Prostaglandin F2alpha produced by inducible cyclooxygenase may contribute to the resolution of inflammation. *Inflammopharmacology* **2005**, *12* (473−476), 477−480.
(39) Smith, D. A.; Di, L.; Kerns, E. H. The effect of plasma protein binding on in vivo efficacy: misconceptions in drug discovery. *Nature Rev. Drug Discovery* **2010**, *9*, 929−939.
(40) Liu, J. F.; Kaselj, M.; Isome, Y.; Ye, P.; Sargent, K.; Sprague, K.; Cherrak, D.; Wilson, C. J.; Si, Y.; Yohannes, D.; Ng, S. C. Design and synthesis of a quinazolinone natural product-templated library with cytotoxic activity. *J. Comb. Chem.* **2006**, *8*, 7−10.
(41) Klapars, A.; Huang, X.; Buchwald, S. L. A general and efficient copper catalyst for the amidation of aryl halides. *J. Am. Chem. Soc.* **2002**, *124*, 7421−7428.
(42) Bradford, M. M. A rapid and sensitive method for the quantitation of microgram quantities of protein utilizing the principle of protein−dye binding. *Anal. Biochem.* **1976**, *72*, 248−254.
(43) Thoren, S.; Jakobsson, P. J. Coordinate up- and down-regulation of glutathione-dependent prostaglandin E synthase and cyclo-oxygenase-2 in A549 cells. Inhibition by NS-398 and leukotriene C4. *Eur. J. Biochem.* **2000**, *267*, 6428−6434.
(44) Schmidt, R.; Coste, O.; Geisslinger, G. LC-MS/MS-analysis of prostaglandin E2 and D2 in microdialysis samples of rats. *J. Chromatogr., B: Anal. Technol. Biomed. Life Sci.* **2005**, *826*, 188−197.
(45) Revermann, M.; Barbosa-Sicard, E.; Dony, E.; Schermuly, R. T.; Morisseau, C.; Geisslinger, G.; Fleming, I.; Hammock, B. D.; Brandes, R. P. Inhibition of the soluble epoxide hydrolase attenuates monocrotaline-induced pulmonary hypertension in rats. *J. Hypertens.* **2009**, *27*, 322−331.